J. COMBIN. MATH. COMBIN. COMPUT. 127a (2025) 5125--5148

Journal of Combinatorial Mathematics and Combinatorial Computing
www.combinatorialpress.com/jcmcc

Combinatorial Press

Study on the accurate calculation method for the distribution of structural residual bearing capacity during the demolition process of the Clearwater River Bridge

Changzhu Wang[1], Jixiang Chai[1], Hongtu Xu[1], Zhiquan Liu[2,✉]

[1] *CCCC Third Highway Engineering CO., LTD., Beijing, 050000, China*

[2] *Bridgee Engineering Consulting of Shanghai, Shanghai, 200084, China*

ABSTRACT

Bridges as the basic transportation facilities in the national daily life, with the development of road transportation, the number of urban viaducts and cross-sea bridges grows year by year, and the role of bridges in the transportation network becomes more and more significant. The article selects the Qingshuihe Bridge demolition project as the research object, and designs the Qingshuihe Bridge demolition implementation program based on the engineering characteristics. For the mechanical property changes and structural residual bearing capacity calculation during the demolition process of Qingshuihe Bridge, this paper constructs a finite element model of Qingshuihe Bridge based on ANSYS software, and analyzes the structural reliability of Qingshuihe Bridge after the demolition project by combining with structural reliability indexes. Under the same mid-span displacement condition, the cracking load error between the finite element simulation values and the experimental values is relatively small, and its fluctuation range is between 2.12%% and 6.58%. In the first 5 years after the demolition of the bridge section, the residual load capacity of the bridge structure increased from 5.23*103kN to 5.51*103kN. The reliability index value of the bridge over the Qingshui River changed relatively slowly in the early stage, and began to decline gradually in the later stage, and the greater the strength of the steel girders the higher time-varying reliability index of the bridge over the Qingshui River. In this paper, the design of the Qingshui River bridge demolition implementation program has a strong feasibility, in order to ensure that the Qingshui River bridge structural residual bearing capacity on the basis of the completion of the demolition of part of the bridge abutment, and can guarantee the safety of the bridge operation.

Keywords: residual bearing capacity, ANSYS software, finite element model, structural reliability

1. Introduction

As the left span of the old bridge over the Qingshui River Bridge does not meet the requirements of the

✉ Corresponding author.
E-mail address: liuzhiquan2005@126.com (Z. Liu).
Received 03 March 2024; Revised 20 April 2024; Accepted 10 November 2024; Published Online 15 April 2025.
DOI: 10.61091/jcmcc127a-289

waterway needs to be demolished and rebuilt, the right span of the bridge for the separation of the additional, with the completion of the right span of the new bridge, the left span of the old bridge formally started to dismantle. Due to the demolition of the bridge in the process of the explosive load caused by the bridge will cause serious damage to the bridge, will not only cause huge economic losses, but also a serious threat to the safety of traffic [1-3]. And in the case of dynamic loads generated during bridge demolition, the mechanical properties of materials exhibited by the building structure or its components are significantly different from those under static loads [4-8]. The bridge deck of the Clearwater River Bridge is mainly made of orthotropic anisotropic steel plates, which have the advantages of light deadweight, high bearing capacity, and fast construction [9]. When the impact load is applied to the steel structure, it will trigger a high strain in the material in a short period of time, and this phenomenon is known as high strain rate [10-11]. In the process of the structure subjected to dynamic loading, the dynamic mechanical properties of steel are significantly different from those in the static state, and the relationship between its stress and strain becomes more complex [12-14]. The change of strain rate will make the relationship between stress and strain of the material become more complicated and lead to significant changes in its key mechanical properties such as strength and elastic modulus [15-17]. Therefore, in the field of engineering, it is crucial to study the simulation study of damage and residual bearing capacity of structures or members under the influence of dynamic loading.

In order to ensure the safety of bridge demolition, it is necessary to reasonably plan the bridge demolition project and strictly control the construction process of bridge demolition, so as to better ensure that the residual bearing capacity of the bridge meets the specification requirements. This paper takes the Qingshuihe Bridge reconstruction and expansion project of Wuxuan WX-03 as the research object, and establishes a finite element model through ANSYS software to analyze the change of bridge force under the demolition and implementation plan of the Qingshuihe Bridge, and discusses the residual bearing capacity of the structure and the interface slippage after the bridge demolition. Combined with the structural reliability index, the JC method is used to solve the structural reliability change of Qingshuihe Bridge after dismantling, which provides accurate calculation results to ensure the stable operation of Qingshuihe Bridge after dismantling part of the bridge piers.

2. Design of the implementation program for the demolition of the Clearwater River bridge

With the rapid development of urban infrastructure, some of the existing roads built in the early days in terms of headroom, span and other aspects have not been adapted to the current urban development and people's travel needs, some of the old bridges in the demolition of the existing line across the existing line, involving the safety of the existing line below, the construction is difficult, and the traditional dismantling, crushing and demolition methods are time-consuming, low efficacy. Therefore, exploring efficient and practical bridge demolition program for the protection of the surrounding environment, reduce the construction difficulty has a very important research significance. Based on this, this paper takes the demolition project of Qingshuihe Bridge as the research object, and explores a kind of efficient bridge demolition program to better ensure the remaining bearing capacity of the bridge structure.

2.1. Summary of works

2.1.1. General overview. Wuxuan WX-03 standard section start and end pile number for K323+650 ~ K341+167.373, along the route through the islet town of Wuhu City islet area, the islet town of the islet area of the islet area of the six towns, Hatue District, in the six Lang hub and Liwu high-speed cross, the end is located in Hatue District of Wuhu City, Hatue District, Wuhu hub, Wuxuan high-speed and the main line of the G4211 Ningwu high-speed intersection. The total length of the route is

17.517km, among which, the length of the reconstruction and expansion section is 16.37km, fully utilizing the proposed reconstruction and expansion of the G4211 Ningwu Expressway Wuhu Hub K340+020.898 ~ K341+167.373 section of a total of 1.146km. The main construction content includes roadbed engineering, pavement engineering, bridge engineering (new construction, alteration, dismantling and maintenance and reinforcement), traffic safety and landscaping, etc. The contract period is 36 months. The contract duration is 36 months. One of the node project for the Qingshui River Bridge, using the original bridge demolition and reconstruction for the left, the right side of the separation of the new for the right program. The bridge superstructure is prefabricated small box girder + (40+66+40) m steel box combination girder + (3×40) m steel box combination girder + (178+85) m steel tie arch + prefabricated small box girder. In the substructure of the bridge, the main pier is column pier, the bearing platform is connected with group pile foundation, the approach pier is pile pier, the abutment is ribbed plate, the bearing platform is connected with group pile foundation, and the total length of the bridge is 1345m.

Figure 1 is the general layout of the main bridge of Qingshui River Bridge. The main bridge is a single-span under-bearing steel box tie arch bridge, the main bridge span arrangement for 178+85m, the main bridge length is 263m, two-span simply supported steel box under-bearing continuous tie arch bridge. 178m across the main channel, 85m across the north side of the embankment. The single bridge cross-section arrangement is 2m (anchor zone) +0.5m (guardrail) +19.25m (carriageway) +0.5m (guardrail) +2m (anchor zone), single width 24.25m. According to the progress of the project and the requirements of the construction drawings, it is necessary to dismantle the existing bridge over the Qingshui River, so as to follow up the construction of the new bridge.

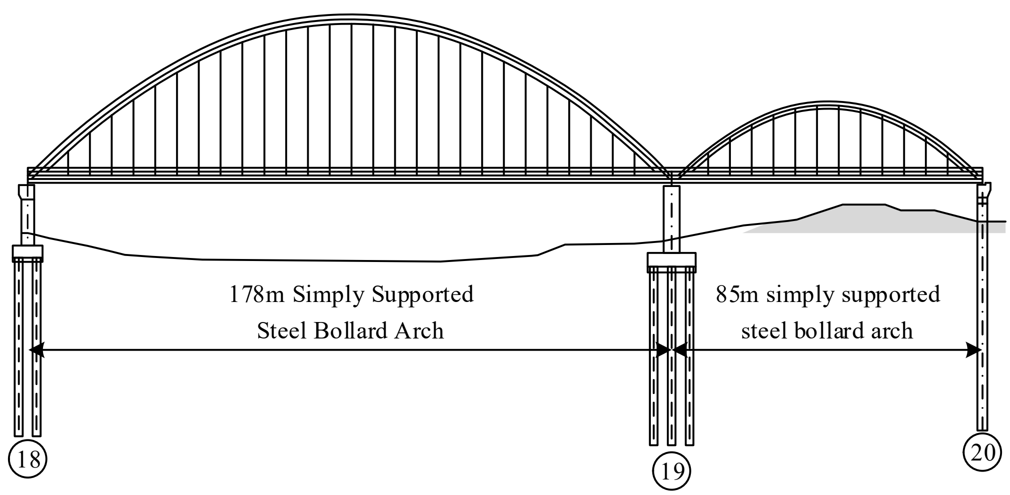

Fig. 1. The main bridge of the main bridge of the Qingshuihe river

2.1.2. Overview of bridges:

1) The main bridge superstructure type of Qingshui River Bridge adopts variable cross-section continuous box girder, the span combination is (30+9x52+30) m, of which the span of navigational tie is 52 m, and the aperture of both sides across the embankment is 52 m. The box girder cross-section is a single box with a single chamber, and the full width is 12.75 m. The height of root girder is 2.8 m. The height of central girder is 1.5 m, and the height of girder is varied according to the paraboloid, and the width of the box girder top plate is 12.75 m. The width of bottom plate is 5.0 m. The longitudinal slope of bridge deck is 1.9%, and the one-way cross slope is 2%. The width of box girder top plate is 12.75m, the width of bottom plate is 5.0m, the longitudinal slope of bridge deck is 1.9%, the one-way transverse slope is 2%, and the transverse slope of bridge deck is adjusted by the height of web plate. The substructure adopts light reinforced concrete perimeter column type single column piers, in order to reduce the piers and columns too much and water blockage, up and down the bridge piers and

columns staggered arrangement. Column diameter is 2.2 meters. Solid bearing platform, bored pile foundation, pile diameter of 1.5 m. Main bridge across the Qingshui River, belongs to the Wutai Canal, navigational standards for V3, according to the Ministry of standard navigable clear width 28-30m, clear height of not less than 5 m. Navigable main channel bias Wuhu bank, the river and the route of the centerline of the angle of 61 °. Qingshui River Approach Bridge, the river and the route of the centerline of the angle of 61 °.

2) The upper structure of Qingshui River Approach Bridge adopts simple-supported and then continuous prestressed concrete precast box girder, with the standard span diameter of 30m. In order to adjust the span diameter difference due to diagonal intersection, a 22.50m bridge span is set up for each of the left and right widths respectively. The right north bank approach bridge abutment span combination is 3x (4x30) m, the south bank is (22.5+3x30) m+(4x30) m, the left north bank approach bridge span combination is 2x (4x30) m+(22.5+3x30) m, the south bank is 2x (4x30) m. The substructure adopts double bridges, supporting the wall-type abutments, the diameter of the abutment columns is 1.4m, the diameter of the piles is 1.5m, the diameter of the pile is 1.0m, and the diameter of the abutments is 1.0m. 1.0m.

2.1.3. Engineering features:

1) The project is located in the urban area around the road, traffic flow, civilized construction, safety and environmental protection requirements, to the project implementation of the greater impact.

2) Clearwater River bridge navigation hole demolition, according to the bridge structural safety and floating crane ship lifting weight of different working positions to accurately divide the cutting beam end, reasonable arrangement of the construction sequence.

3) Qingshui River is busy with shipping, and navigation conditions need to be fully ensured during the demolition process.

4) During the construction process, there are more secondary pollution such as noise, waste water, dust, etc., and the pressure on environmental protection is greater.

5) The bridge demolition for the left width of the bridge construction of the pre-process, in order to ensure the smooth progress of the subsequent projects, bridge demolition construction need to strictly control the duration of the construction period, careful arrangement of construction plans.

2.2. Implementation Program

2.2.1. Dismantling process. Qingshui River Bridge is the controlling project of this project, and its main bridge is (30+9x52+30)m continuous box girder bridge, cast-in-suspension bridge, with staggered arrangement of left and right widths, of which the 16th and 17th spans are navigable holes. The demolition of the bridge should fully consider the impact of navigation under the bridge, using the window period of the waterway, to minimize the impact on the waterway under the bridge. In 2010, the bridge was strengthened by thickening the web after prestressing for the diagonal cracks in the web, and at the same time, the abutments were strengthened by enlarging the cross-section. The demolition of the bridge should fully consider the structural characteristics of the old bridge to ensure the structural safety and stability of the old bridge in the demolition process. In addition, the demolition work should fully consider the impact on the surrounding environment, water bodies, etc., to meet the relevant norms, standards and thematic results. On the basis of ensuring safety, combined with the structural characteristics of the bridge and the demand for navigation, the demolition of the old bridge is carried out in a scientific and reasonable manner to improve the construction efficiency.

Figure 2 shows the demolition process of the main bridge. Considering the site conditions, in order to reduce the impact on the waterway, after the piers are added with temporary consolidation measures, it is proposed to choose the unsupported method of demolition of the old bridge, the demolition work is concentrated in the window period of the waterway, in order to improve the dismantling efficiency, the use of rope saws to cut, and floating cranes for transportation. Centralized pile in the big pile number side of the river rover for crushing, clearing. The rest of the main bridge across the river in the dry season are rambling, with large-scale machinery into the field operating conditions, according to the site construction needs and construction technology, choose the machine drilling method for demolition, a single left and right of each arrangement of 8 sets of 27m lengthened arm rock drill symmetrically crushed box beams. Considering that the old bridge on the left is close to the new bridge, in order to avoid the girder collapsing and tumbling and endangering the safety of the new bridge abutment, lattice brackets are set up at the bottom of the girder on the right 18-21 spans to protect it.

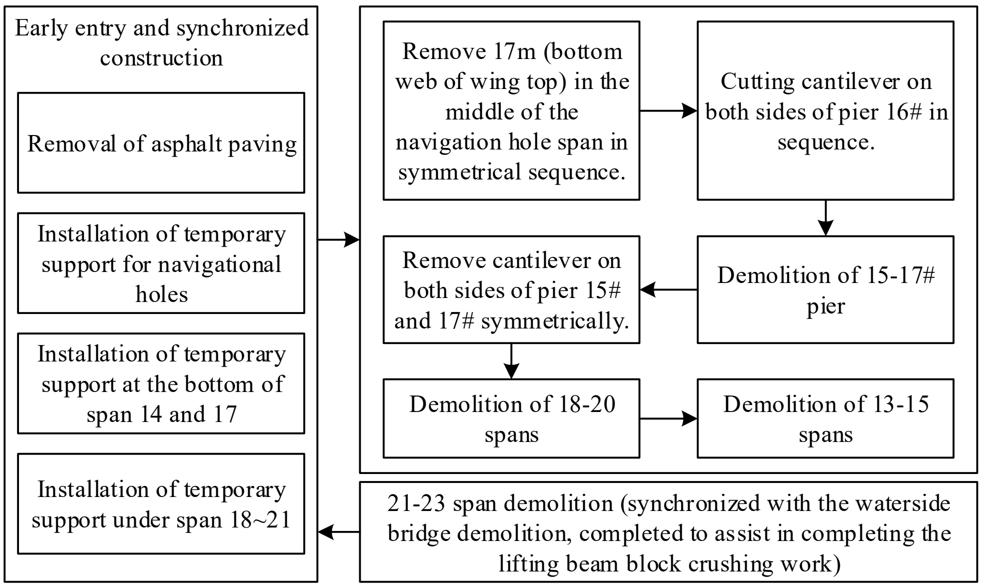

Fig. 2. Main bridge removal process

Figure 3 shows the demolition process of the south and north approach bridges. The south and north approach bridges are prestressed combined box girder structures, with smaller girder spans and widths and heights, and also with machine chiseling operating conditions. The crusher is used for direct crushing, and the dismantled concrete components and waste materials are loaded into trucks with excavators and loaders to be transported to the surrounding stockpile area for uniform treatment.

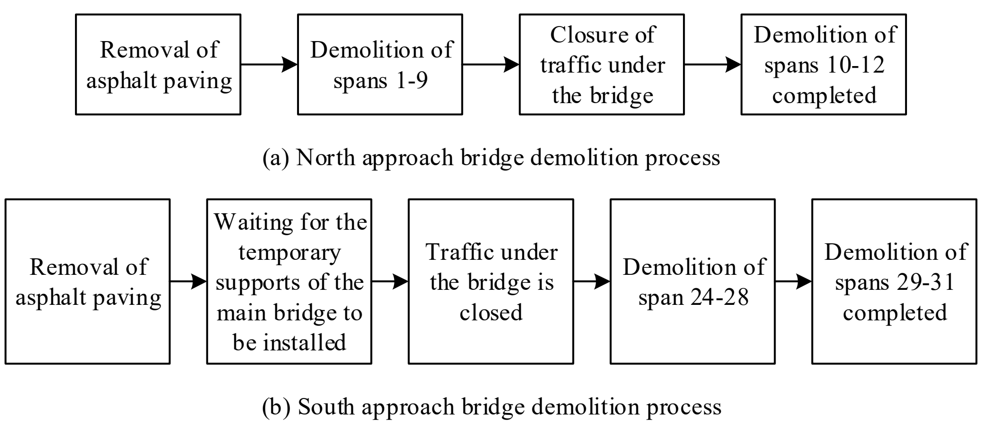

Fig. 3. South, North bridge demolition process

2.2.2. Dismantling program. The demolition of the old bridge was carried out in accordance with a top-to-bottom demolition sequence, starting with the removal of the paving layer of asphalt concrete, followed by the demolition of the superstructure, and ending with the demolition of the substructure. According to the respective bridge structure and site conditions of the differences, the three work surfaces of the bridge demolition work are coordinated.

1) Bridge deck pavement demolition. The thickness of the bridge deck paving layer of asphalt concrete is 9cm, which is milled by milling machine and transported away by truck. The thickness of bridge deck concrete paving layer is about 9cm, and the paving layer concrete is broken in situ with the beam body.

2) Collision guardrail removal. Inside the waveform beam guardrail every 4.0m section, with a car crane + 1t sling lifting guardrail piece, oxygen cutting its roots and beams, and then loaded to the truck transfer out of the field, and resource utilization. The outer New Jersey guardrail is divided into two cases, the outer guardrail of the waterside portion of the main bridge of the Clearwater River Bridge is cut and lifted together with the unit block for off-site crushing, and the outer guardrail of the rest of the bridge is crushed in-situ together with the girders.

3) Removal of the superstructure of the waterside section of the main bridge of Qingshuihe Bridge. As a whole, 16#, 15#, 17# piers as the center of the symmetrical demolition, considering the continuous beam bridge span lifted on the adjacent span of the adverse effects and the bridge appeared in the original disease, the first lifting of the span section 1 length of 17.0m, the total weight of the section is 363.9 tons. Near 16#, 15#, 17# piers for section 2, section length 14.45m, section total weight of 422.6 tons (including the box after pouring high strength grout). The top position of pier is section 3, section length is 3.5m, section weight is 103.3 tons. Near pier 15# and 17# is section 2-X, length is 3.75m, section weight is 81 tons.

4) Clearwater River bridge main bridge water section substructure demolition. 15 ~ 17 # pier is located in the waterway, to be demolished after the upper part of the main girder can begin to pier above the water surface part of the rope saw cutting and lifting. Considering the needs of waterway protection, the piers in the water area are cut and lifted away from the site in pieces. Piers demolition of the upper structure has been demolished, floating crane boom elevation angle is no longer restricted by space, the rated lifting weight can be increased to 196t. Planned rope saw cutting 3 times will be divided into 3 pieces of piers, vase piers on the upper part of the changes in the section is divided into equal weight of the two pieces, the lower part of the equal width of the section in the center of the position of the two into two sub-assembled lifting. Take the heaviest right 15# pier as an example, the largest block weight 98.35t. Waterside pier bearing and piling, according to the actual situation on site, need to be demolished to the riverbed line below 1.0m. The underwater part of the proposed use of the gun head machine station barge to directly carry out in-situ crushing operations and then slagging. According to the requirements of the waterway department, broken to the riverbed below 1.0m elevation, after mapping to meet the requirements of the end of the main bridge waterside section of the demolition operation.

5) Clearwater River Bridge main bridge land section demolition. The land section of the main bridge is divided into two parts, the 13th-15th span and the 18th-23rd span by the navigable hole. Among them, spans 13-15 cross the north bank embankment, spans 18-21 are river flooding section (no water during construction season), and spans 21-23 cross the south bank embankment, all of which are located on the land, with good working conditions, and can be dismantled directly by rock drilling method. The demolition work on the north side started from span 15, and the demolition work on the south side started from span 23. In view of the spacing between the two bridges is only 50cm, in order to provide the construction work surface, the flange plates were firstly broken on the bridge deck. Four crushers were arranged on each span of the bridge to synchronize the chiseling of the flange plates.

6) Demolition of Qingshuihe Bridge Approach Superstructure. The approach bridge of Qingshuihe Bridge adopts 30m prestressed concrete combined box girder, first simply supported and then continuous structure, transversely arranged 4 pieces of girders, with wet joints of 75cm. the approach bridge is located on the bank, and the proximity of the air is low, which is convenient for the crusher to be positioned on the side of the bridge to carry out the crushing directly. Each span is arranged with

3 crushers, and the left and right widths are arranged symmetrically, crushing the girders one by one. The crushed slag directly falls under the bridge, and the residual reinforcement and prestressing steel bundles are cut off by hydraulic shears and then fall down.

7) Demolition of the substructure of the approach bridge of Qingshuihe Bridge. The demolition of substructure should follow the principle of top-down step by step. First remove the platform cap, then remove the cover beams, pier columns (platform), and finally remove the foundation part of the bearing platform. Removal should be noted that the radius of operation of the machinery should be greater than the height of the pier. Crusher from top to bottom gradually bridge deck, pier and column broken, encountered when the rebar connection can be cut using oxygen acetylene, when the machine chiseling and crushing fallen concrete block is large, in order to save time, you can use the excavator or loader loading, transported to the stockpile area, and then use the crushing hammer to change the small.

3. Calculation model of the residual bearing capacity of the demolished structure of the Clearwater River bridge

With the development of the times, some bridges have accumulated a large number of disease problems due to the long operation time. In order to better meet the growing traffic demand, it is urgent to take measures of reconstruction and expansion. Bridge demolition project is a difficult point in the highway expansion project, which has a significant impact on the overall quality of the expansion project. In the actual construction process, the relevant personnel need to strictly follow the principle of safety first, the use of whole to zero way, improve the rationality of the demolition program. At the same time, under the limitation of the conditions of construction while passing through the traffic, it is necessary to combine the characteristics of the project and take effective measures to improve the construction safety and ensure the safety and smooth progress of the project. Based on this, this paper intends to simulate and calculate the structural residual bearing capacity and reliability of the Qingshuihe Bridge demolition process through the finite element model to ensure the safety and efficiency of the Qingshuihe Bridge demolition process, and at the same time, protect the ecological environment, reduce the impact on the surrounding area, and promote the rational use of resources to achieve a win-win situation for both economic and social benefits.

3.1. Material Dynamic Properties and Intrinsic Modeling

3.1.1. Concrete material model

1) Concrete material constitutive model. In the finite element numerical simulation analysis, the concrete constitutive relationship considers the effect of softening after the material reaches plasticity. The modulus of elasticity and Poisson's ratio of concrete are the main parameters describing the elastic behavior of the material, and the Code stipulates the values to be taken. In ANSYS finite element numerical analysis, the damage plasticity model is used for the concrete principal structure. Concrete is subjected to continuous damage, and the gradual accumulation of damage causes the emergence and development of microcracks, and the stress-strain relationship of concrete exhibits nonlinear characteristics, so the damage plasticity model (CDP) can be used to better simulate the change of its properties with material deterioration [18]. In the CDP model, concrete stiffness degradation can be defined by the stiffness damage factor parameter. The uniaxial compressive stress-strain relationship of concrete is computationally expressed as:

$$\sigma_c = \left(1 - d_c\right) E_0 \left(\varepsilon_c - \varepsilon_c^{pl}\right) \tag{1}$$

The calculated uniaxial tensile stress-strain relationship for concrete is expressed as:

$$\sigma_t = \left(1 - d_t\right) E_0 \left(\varepsilon_t - \varepsilon_t^{pl}\right) \tag{2}$$

Where, σ_c is the concrete compressive stress, ε_c is the total concrete compressive strain, ε_c^{pi} is the elastic compressive strain of concrete without damage, d_c is the concrete compressive damage factor, σ_t is the concrete tensile stress, ε_t is the total concrete tensile strain, ε_t^{pt} is the elastic tensile strain of concrete without damage, d_t is the concrete tensile damage factor.

The main parameters of the concrete damage plasticity model are expansion angle ψ, flow potential offset η, biaxial compression and uniaxial compression ultimate strength ratio σ_{b0}/σ_{c0}, invariant stress ratio K_c, viscous coefficient μ.

2) Concrete Damage Criteria. The current damage theory usually assumes that concrete satisfies the assumption of isotropy before damage, and the damage equation can be expressed in coordinates ζ, r, θ. The expression is:

$$f\left(\xi, r, \theta, k_1, k_2, \cdots, k_n\right) = 0 \tag{3}$$

where $k_1, k_2, \cdots, k_m$ is a constant to be determined and ξ, r, θ is the Haigh-Westegaard coordinate. Then:

$$\xi = \frac{1}{3}\left(\sigma_1 + \sigma_2 + \sigma_3\right) = \frac{1}{\sqrt{3}} I_1 \tag{4}$$

$$r = \sqrt{2J_2} = \frac{1}{\sqrt{3}}\left[\left(\sigma_1 - \sigma_2\right)^2 + \left(\sigma_2 - \sigma_3\right)^2 + \left(\sigma_3 - \sigma_1\right)^2\right]^{\frac{1}{2}} \tag{5}$$

$$\cos\theta = \frac{2\sigma_1 - \sigma_4 - \sigma_3}{\sqrt{2}\left[\left(\sigma_1 - \sigma_2\right)^2 + \left(\sigma_2 - \sigma_3\right)^2 + \left(\sigma_3 - \sigma_1\right)^2\right]^{\frac{1}{2}}} \tag{6}$$

The three-dimensional three-dimensional drawing of the damage envelope surface is inconvenient to draw, in order to facilitate the representation, usually with the section of the damage surface intersecting with the bias plane and the meridian of the damage surface to express. The bias plane envelope is triple fold symmetry, and the tensile meridian is the plane formed by the hydrostatic pressure axis and a line at an angle to the damage surface, which intersects with the damage surface and becomes a curve. According to many concrete test data, summarized several important characteristics of the damage surface of concrete:

(1) The damage surface is continuous, smooth, convex, and triple-fold symmetrical to the hydrostatic pressure axis.

(2) hydrostatic pressure for tension or smaller pressure, the cross-section on the skewed surface is approximately triangular, with the increase of hydrostatic pressure, the cross-section gradually tends to circular.

(3) The value of y of the meridian increases with goodness, but tends to level off. When the hydrostatic pressure is pressure, the hydrostatic pressure axis will not intersect the damage surface, i.e., concrete under triaxial isobaric compressive stress will not be damaged.

(4) The longitudinal coordinate at tensile meridian ($\theta = 0°$) is represented by r_t, and the grade coordinate at compressive meridian ($\theta = 60°$) is represented by r_c. r_t/r_c increases with hydrostatic pressure but is always less than 1. When $\xi = 0$, $r_t/r_c \approx 0.5$.

The damage criterion model for concrete strength is based on the Bresler-Pister three-parameter criterion in this paper [19]. This criterion assumes that the partial section is taken as a circle and the meridian is a quadratic parabola, which can be expressed as:

$$\frac{\tau_0}{f_c} = a - b\frac{\sigma_0}{f_c} + c\left(\frac{\sigma_0}{f_c}\right)^2 \tag{7}$$

Where σ_0 is the octahedral positive stress, $\sigma_0 = \frac{1}{3} I_1$, I_1 is the first invariant of stress, τ_0 is the octahedral pre-stress, $\tau_0 = \sqrt{\frac{2}{3} J_2}$, J_2 is the second invariant of bias stress, a , b , c is determined by the uniaxial tensile and compressive strengths f_t, f_c bi-directional compressive strengths f_{cb}.

3.1.2. Reinforcing steel material model. A MAT-Plastic-Kinematic bilinear elastic-plastic model with attendant reinforcement is used to simulate the elastic-plastic behavior of the reinforcing steel material during bridge demolition, and the effect of strain rate is also considered. The system automatically deletes the units of this model when the unit failure strain value is out of the preset range in order to simulate the fracture failure of steel bars [20]. The reinforcement bar yield strength is determined by the parameters provided in the following equation, and the variation of these parameters will directly affect the mechanical properties of the steel expressed as:

$$\sigma_y = \left[1 + \left(\frac{\dot{\varepsilon}}{C}\right)^{1/p}\right]\left(\sigma_0 + \beta E_p \varepsilon_p^{eff}\right) \tag{8}$$

where σ_0 is the initial yield strength of the reinforcement, σ_y is the dynamic yield strength of the reinforcement, β is the elastic-plastic hardening parameter, $0 < \beta < 1$, ε is the material strain rate, and C , p are the material constants.

The plastic hardening modulus E_p can be expressed as:

$$E_p = EE_t / \left(E - E_t\right) \tag{9}$$

where E is the initial elastic modulus and E_t is the plastic tangent modulus.

3.2. Model Construction and Boundary Condition Design

3.2.1. ANSYS software. ANSYS software is a large-scale general-purpose finite element analysis software integrating structural, fluid, electromagnetic, acoustic and thermal analysis, which is the only computer-aided engineering (CAE) design and analysis software in FEM analysis that has passed the ISO9001 quality certification to date.ANSYS software mainly contains pre-processing module, analysis and calculation module and post-processing module of these three parts. The functions of the pre-processing module mainly include solid modeling, meshing, applying loads. The analysis module is the computational kernel of ANSYS, i.e. the solver, which provides different solvers for different problems. The post-processing model is mainly to view the computational results of the model, which can be used to display the results required by the calculator in the form of color clouds, lists, and defined paths [21].

ANSYS software can be used to simulate the relaxation of prestressing tendons of bridges, cracking and shrinkage creep of concrete, compression collapse, and temperature changes in the structure and other factors on concrete bridge members, but also effectively calculate the shear hysteresis effect of concrete bridges under the action of the load, aberrant stresses, and concrete contact, and so on, and so the current simulation of the safety process of the concrete members if the The unit model provided by ANSYS is more effective and credible. ANSYS software has become the mainstream software for finite element analysis and calculation in civil engineering, machinery and other industries because of its powerful analytical functions.

3.2.2. Numerical modeling. ANSYS software is used to establish the whole bridge finite element model of the cast-in-place box girder demolition bridge over the Qingshui River, and the model is established by the beam lattice method, with a total of 1,216 nodes and 1,011 units, and the finite element model of the bridge over the Qingshui River is shown in Figure 4. In order to simulate the real condition of the scene, and the complete establishment of the temporary support columns of pier 16#, according to the actual boundary conditions of the nodes for constraints, to cast-in-place box old bridge dismantling cross-section after the remaining box girder load on the force of the support system for the check.

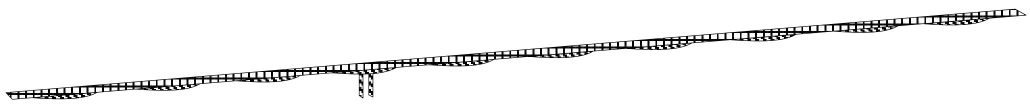

Fig. 4. The finite element model of Qingshuihe bridge

The gravity density of the concrete is 26.0kN/m3, the modulus of elasticity is 3.45×104MPa, the surface load is taken as 2.34kN/m2, and the wind load is calculated according to the “Design Code for Highway Bridges Resistant to Wind”.

3.2.3. Boundary condition settings. The background combined girder bridge is simulated by solid unit and truss unit, the concrete deck slab, steel girder, and mat are simulated by unit solid C3D9R, and the reinforcement etc. and support are simulated by truss unit, and the effect of shear and the slip of each component is generally ignored in modeling, and a simplified model is used to reduce the calculation amount. The finite element model consists of neighboring cell nodes connected to each other to form a whole, using the cell stiffness matrix to run the calculation. The mesh size is related to the normal operation of the model. Since the main analysis of the model is the change of load on the plate surface, the mesh is refined to prevent the local cell mesh from yielding prematurely and causing the end of the calculation.

According to the selected background in-service bridge, set the finite element constraint method, the finite element model of the concrete slab, steel girder and other components are established separately, and then the above components are assembled and the contact method is set, the transverse and longitudinal reinforcement bars are established first, and then merged into a whole, and then embedded into the plate unit, the pads are used to simulate the wheels are loaded on the bridge deck plate surface, and the bottom of the steel girder is cemented. In order to avoid sliding of the loading pads and the slab surface, the connection method also adopts cementation, and the coupling between the point and the opposite side is used for constraint, and the displacement loading method is used for loading.

3.3. Calculation Methods for Structural Reliability of Bridges

3.3.1. Structural reliability indicators. Since the reliability and unreliability of the structure is unpredictable during the construction and use of the structure, but under normal use conditions, the reliability of the structure can be estimated by the degree of reliability, and the design approach that meets the code requirements of the reliability index can be put into the actual structure.

Structural reliability is a probabilistic measure of structural reliability. The probability of reliability is denoted by p_r and the probability of failure by p_f. The following relationship is satisfied:

$$p_r + p_f = 1 \tag{10}$$

The structure function function Z is a continuous random variable, and let the probability density function of Z be $f_z(z)$. The significance of the probability of reliability and the probability of failure follows:

$$p_r = P_r(Z > 0) = \int_0^{+\infty} f_Z(z)dz \tag{11}$$

$$p_f = P_r(Z \le 0) = \int_{-\infty}^{0} f_z(z)dz \tag{12}$$

When the joint probability density function of the random variable $X = \left(X_1, X_2, \cdots, X_n\right)^T$ is $f_x(x) = f_x\left(x_1, x_2, \cdots, x_n\right)$ and the joint cumulative distribution function is $F_X(x) = F_X\left(x_1, x_2, \cdots, x_n\right)$, then:

$$\begin{aligned} p_f &= \int_{z\le 0} dF_x(x) = \int_{z\le 0} f_X(x)dx \\ &= \int \cdots \int_{z\le 0} f_X\left(x_1, x_2, \cdots, x_n\right) dx_1 dx_2 \cdots dx_n \end{aligned} \tag{13}$$

If each X_i is independent of each other and the probability density function of X_i is $f_{x_i}\left(x_i\right)$, then:

$$p_f = \int \cdots \int_{z\le 0} f_{X_1}\left(x_1\right) f_{X_2}\left(x_2\right) \cdots f_{X_n}\left(x_n\right) dx_1 dx_2 \cdots dx_n \Big] \tag{14}$$

The probability of failure p_f is determined primarily by the form of the distribution of the function Z. For a normal random variable Z, denoted $Z \sim N\left(\mu_z, \sigma_z\right)$. Then the probability density function of Z is:

$$f_z(z) = \frac{1}{\sqrt{2\pi}\sigma_z} \exp\left[-\frac{\left(z-\mu_z\right)^2}{2\sigma_z^2}\right] \tag{15}$$

Standard normalization is applied to it. $Y = \left(Z - \mu_z\right)/\sigma_z$, i.e., $Y \sim N(0,1)$, its probability density function and cumulative distribution function are, respectively:

$$\varphi(y) = \frac{1}{\sqrt{2\pi}} \exp\left(-\frac{y^2}{2}\right) \tag{16}$$

$$\Phi(y) = \int_{-\infty}^{y} \varphi(y)dy \tag{17}$$

The expression for the failure probability of the structure at this point is:

$$p_f = \int_{-\infty}^{0} \frac{1}{\sqrt{2\pi}\sigma_z} \exp\left[-\frac{\left(z-\mu_z\right)^2}{2\sigma_z^2}\right] dz = \int_{-\infty}^{\frac{\mu_z}{\sigma_z}} \varphi(y)dy = \Phi\left(-\frac{\mu_z}{\sigma_z}\right) \tag{18}$$

The distance to the mean μ_z of the origin 0 can be measured by the standard deviation σ_z, i.e.:

$$\beta = \frac{\mu_z}{\sigma_z} \tag{19}$$

β is a dimensionless number known as the reliability index of the structure, or reliability index for short, and after calculating the failure probability of the node by Monte Carlo method, the failure probability of the structure can be expressed as:

$$p_f = \Phi(-\beta) = 1 - \Phi(\beta) \tag{20}$$

β is related to the reliability probability p_r as:

$$p_r = \Phi(\beta) \tag{21}$$

The function function $Z = R - S$, assuming $R \sim N(\mu_R, \sigma_R)$, $S \sim N(\mu_s, \sigma_s)$, and since Z is a linear function of R and S, and Z also obeys a normal distribution, $\mu_z = \mu_R - \mu_S$, and $\sigma_z^2 = \sigma_R^2 + \sigma_S^2$, is obtained from the above defined formula for the reliability index:

$$\beta = \frac{\mu_R - \mu_S}{\sqrt{\sigma_R^2 + \sigma_S^2}} \tag{22}$$

3.3.2. Structural reliability calculations. For the non-normal random variable X_i, the mean is μ_{x_i}, the standard deviation is σ_{x_i}, the probability density function is $f_{X_i}(x_i)$, and the cumulative distribution function is $F_{X_j}(x_i)$. For the random variable X_i after equivalent normalization, the variable is X_i', the mean and standard deviation are $\mu_{X_i'}$ and $\sigma_{X_i'}$, and the corresponding probability density function is $f_{X_i'}(x_i')$, and the cumulative distribution | is $F_{X_i'}(x_i')$. When using the JC method to find the reliability index, performing the equivalent normalization should satisfy that the probability density function and the cumulative distribution function at the checkpoints x_i^* at X_i' and X_i correspond equally, i.e:

$$F_{X_i'}(x_i^*) = \Phi\left(\frac{x_i^* - \mu_{X_i'}}{\sigma_{X_i'}}\right) = F_{X_i}(x_i^*) \tag{23}$$

$$f_{X_i'}(x_i^*) = \frac{1}{\sigma_{X_i'}}\varphi\left(\frac{x_i^* - \mu_{X_i'}}{\sigma_{X_i'}}\right) = f_{X_i}(x_i^*) \tag{24}$$

The inverse function of Eq. (23) yields the following equation:

$$\mu'_{X_i'} = x_i^* - \Phi^{-1}\left[F_{x_i}(x_i^*)\right]\sigma_{X_i'} \tag{25}$$

Solved by equation (24):

$$\sigma_{X_i'} = \frac{\varphi\left\{\Phi^{-1}\left[F_{X_i}(x_i^*)\right]\right\}}{f_{X_i}(x_i^*)} \tag{26}$$

For a lognormal random variable X_i, there are:

$$\Phi\left(\frac{\ln x_i^* - \mu_{\ln X_i}}{\sigma_{\ln x_i}}\right) = \Phi\left(\frac{x_i^* - \mu_{X_i}}{\sigma_{x_i'}}\right) \tag{27}$$

From equation (27):

$$\frac{\ln x_i^* - \mu_{\ln x_i}}{\sigma_{\ln X_i}} = \frac{x_i^* - \mu_{x_i^{\cdot}}}{\sigma_{x_i^*}} \tag{28}$$

From equation (24):

$$\frac{1}{\sqrt{2\pi}\sigma_{\ln x_i} x_i^*}\varphi\left(\frac{\ln x_i^* - \mu_{\ln x_i}}{\sigma_{\ln x_i}}\right) = \frac{1}{\sqrt{2\pi}\sigma_{X_i'}}\varphi\left(\frac{x_i^* - \mu_{X_i'}}{\sigma_{X_i'}}\right) \tag{29}$$

From equation (26):

$$\sigma_{x_i'} = x_i^*\sigma_{\ln X_i} = x_i^*\sqrt{\ln\left(1 + \delta_{X_i}^2\right)} \tag{30}$$

Substituting Eq. (25) into Eq. (30) yields:

$$\mu_{x_i'} = x_i^* + x_i^*\left(-\ln x_i^* + \mu_{\ln x_i}\right) = x_i^*\left[1 - \ln x_i^* + \ln\left(\frac{\mu_{x_i}}{\sqrt{1+\delta_{x_i}^2}}\right)\right] \tag{31}$$

The JC method requires equivalent normalization of non-normal random variables. The iterative steps of the JC method are as follows:

1) Assign the initial checkpoint $x^* = \left(x_i^{*(0)}, x_2^{*(0)}, \cdots, x_n^{*(0)}\right)$, which is generally taken as $x^{(0)} = \left(\mu_{X_1}, \mu_{X_2}, \cdots, \mu_{X_n}\right)$ first.

2) Calculate σ_{x_i} and $\mu_{x_i'}$.

3) Calculate β.

4) Calculate $\cos\theta_{X_i}$.

5) Calculate the new check point $x^{*(1)}$.

6) The (1) to (5) will be iterated sequentially, if the difference between the two $\left\|x^*\right\|$ before and after $<\varepsilon$, then terminate the iteration, at this time β for the required reliability index of the structure, otherwise, take $x^{*(0)} = x^{*(1)}$ to (2) to continue the iteration.

4. Simulation calculation of residual bearing capacity of the demolished structure of the Clearwater River bridge

With the rapid development of highway construction, more and more bridges need to be dismantled and rebuilt due to construction quality defects, overloading, aging, planning adjustments, etc. Bridge demolition safety accidents occur from time to time. According to the relevant accident research found that the vast majority of demolition accidents from the demolition process selection is not appropriate, the demolition of the construction safety technology risk understanding is not in-depth, not comprehensive, risk identification and safety measures are not in place. Demolition of bridges and new bridges are inverse processes, construction technology, safety measures have common, but the mechanism of safety risk and the form of expression is different. In order to avoid safety accidents in the demolition project, it is necessary to clarify the reasons for the demolition of bridges, the characteristics of demolition, the structural type of the bridge to be dismantled and mechanical properties, from the perspective of technical safety, systematic and comprehensive understanding of the sources of safety risks of bridge demolition, accordingly analyze the safety risks of the bridge to be dismantled, and design a reliable and applicable demolition program to ensure the smooth implementation of the demolition project.

4.1. Analysis of the force properties during dismantling

4.1.1. Load-displacement curves. Based on the demolition scheme of Qingshuihe Bridge given in the previous section, the experiment simulated in ANSYS software is the demolition scheme of Qingshuihe Bridge. The test adopts three-point loading, the reinforcement in the compression and tension zones of the member is HRB400 steel, the prestressing tendon adopts Φs15.2 (2×8) 1860 grade strand, the distance from the center of gravity to the edge of the beam tensile zone is 80mm, and the tension control stress is taken as 0.7, the thickness of the protective layer of the concrete is 40mm, and the hoop reinforcement is Φ8@100, and the arrangement is in the whole length. In this paper, a total of nine different types of Qingshui River bridge models are designed, and the demolition work of different types of Qingshui River bridges is carried out by the demolition program of Qingshui River bridge given in the previous paper. The load-displacement curves of the bridges in the demolition process are compared with the experimental values, and the comparison results are shown in Fig. 5, and the specific data results are shown in Table 1. Among them, Fig. 5(a)~(i) shows the comparison results of nine different types of Clearwater River bridge models, respectively.

From Fig. 5 and Table 1, it can be seen that before reaching the cracking load, the mid-span load-displacement curves of the finite element simulation values of the nine different types of Clearwater River bridge models and the experimental values almost coincide. However, after cracking the stiffness of the experimental bridges is basically smaller than that of the simulated beams, and the mid-span load-displacement curves of the finite element simulation values no longer coincide with those of the experimental values near 0.55 Fu. Comparatively speaking, the error between the values obtained from finite element simulation and the experimental values of cracking load is relatively small, and its fluctuation range is between 2.12% and 6.58%, and the finite element simulation values of the bridge over the Clearwater River will be slightly lower than the experimental values of cracking load under the same conditions of mid-span displacement. As for the ultimate load of the bridge, the maximum error between the finite element simulation value and the experimental value can be up to 28.89%, which is due to the fact that with the development of the initial cracks in the experimental Clearwater River bridge model, the experimental beams produce initial defects and affect the subsequent stiffness degradation law of the experimental beams. In contrast, ANSYS simulation treats the beams as ideal elastic-plastic entities, and the stiffness degradation is not affected by cracking during the whole loading process. Overall, the use of finite element software can be more intuitive to show the load-displacement situation of the Qingshuihe bridge in the demolition process, to help the construction personnel to understand the load changes brought to the bridge by the demolition project, and to lay the foundation for optimizing the Qingshuihe demolition plan.

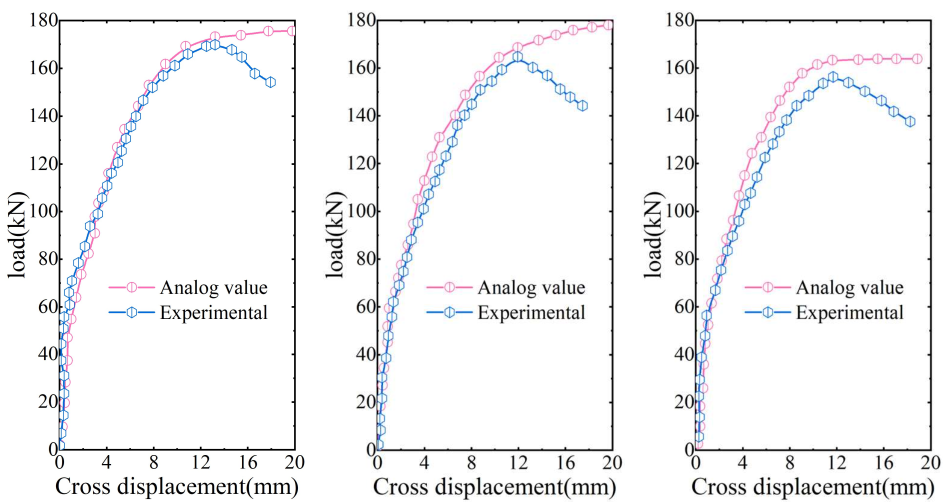

(a) QSH-1 (b) QSH-2 (c) QSH-3

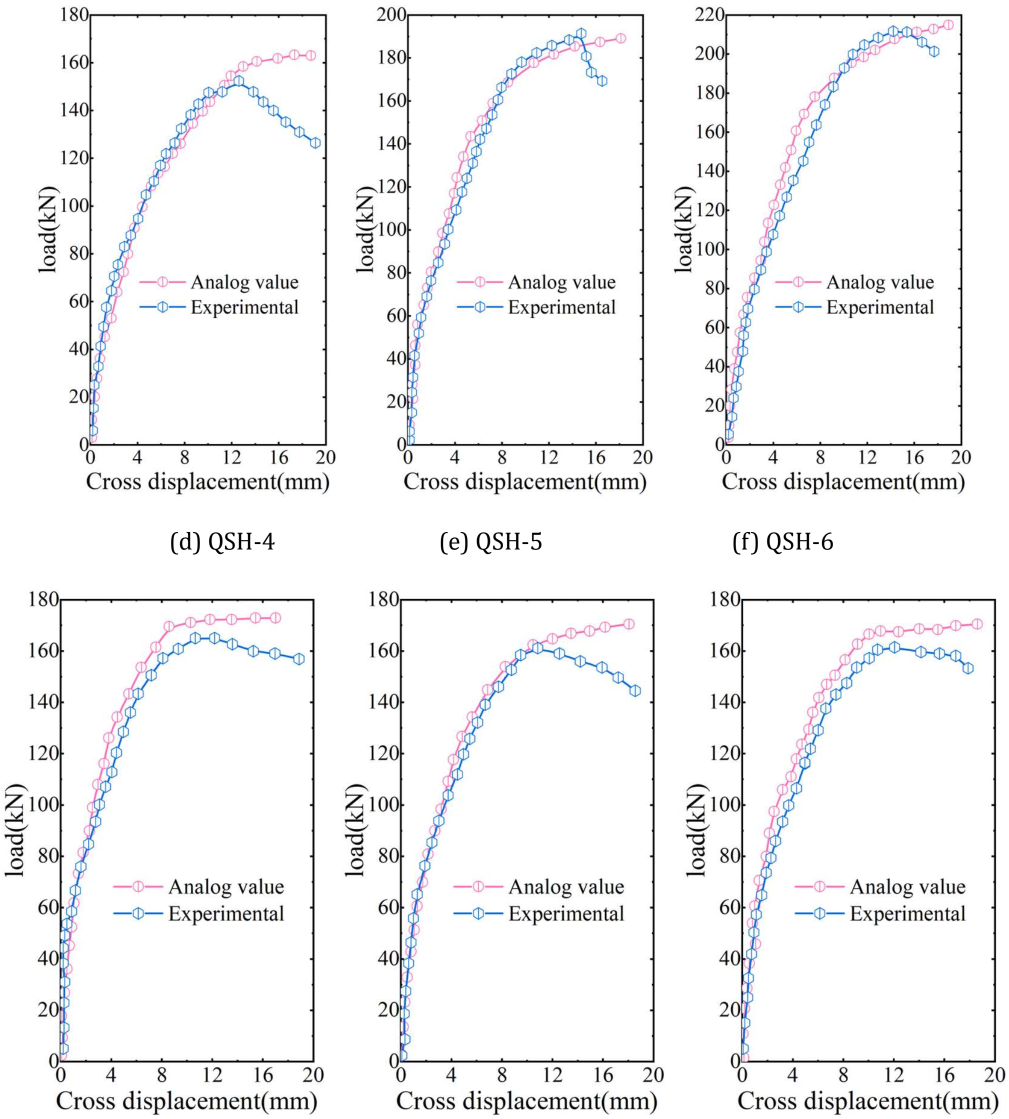

(d) QSH-4 (e) QSH-5 (f) QSH-6

(g) QSH-7 (h) QSH-8 (i) QSH-9

Fig. 5. Comparisons of FEM Calculation Values and Test Values

Table 1. Comparison between experimental and numerical analysis

No.	Cracking load (kN)		Cracking error (%)	Ultimate load (kN)		Ultimate error (%)
	Test	Analog		Test	Analog	
QSH-1	73.06	68.25	6.58	175.56	154.17	12.18
QSH-2	68.24	66.37	2.74	144.19	178.01	23.46
QSH-3	67.41	65.98	2.12	137.57	163.81	19.07
QSH-4	64.32	61.55	4.31	126.41	162.93	28.89
QSH-5	66.15	68.49	3.54	169.27	189.07	11.70
QSH-6	64.26	60.07	6.52	201.32	214.95	6.77
QSH-7	67.31	71.24	5.84	156.87	172.87	10.20
QSH-8	59.86	63.72	6.45	144.49	170.46	17.97
QSH-9	66.39	68.31	2.89	153.25	169.89	10.86

4.1.2. Stress trends. The objective of the stress monitoring is to ensure that the stresses in the control sections of the bridge meet the design requirements during the various stages of the demolition process as well as in the girder segments after the demolition. According to this goal, it is necessary to monitor and analyze the control section stress at different construction stages of the bridge to ensure that the maximum section stress meets the design requirements, so as to ensure the safety of the construction process and to meet the design requirements of the bridge in the state of completion. The dismantling project of Qingshuihe Bridge is symmetrically dismantled with 16#, 15# and 17# piers as the center, and 12 stress monitoring points (P1~P12) are set on the three piers respectively to obtain the stress distribution of 16#, 15# and 17# piers during the construction process. Through the finite element model of Qingshuihe Bridge set up in this paper to simulate the demolition process, and compare the simulation analysis results with the data of stress monitoring in the construction process, we get the stress change trend of the girder segments in the construction process of Qingshuihe Bridge as shown in Figure 6. Among them, Fig. 6(a)~(b) shows the cross-section stress change trends of the superstructure and substructure of the watershed section of the main bridge of Qingshuihe Bridge, respectively.

Based on the finite element analysis software for 16#, 15#, 17# girder segments of the whole process of demolition and construction analysis, it can be obtained that the lower structure of the waterside section of the main bridge of the Qingshuihe Bridge is basically in the full cross-section pressurized state during the bearing process and the value of the cross-section positive stress increases with the progress of construction, and its shear stress increases with the progress of construction. Through the comparison and analysis of the field measured values and finite element simulation results, the study shows that the field measured values and the finite element calculated values have a large deviation in individual stress points, the maximum of which reaches 15.77%, which may be related to the field construction loads and testing environment. The overall deviation is about 10.5%, which can meet the engineering needs. And from the Qingshuihe Bridge main bridge 16 #, 15 # and 17 # of the three piers of the stress trend, the construction process to carry out symmetrical demolition of the three piers is feasible, can effectively ensure that the Qingshuihe Bridge on both sides of the stress trend tends to be the same, to better ensure the stability of the bridge, even if part of the piers withdrawn will not cause the phenomenon of Qingshuihe Bridge suddenly collapsed.

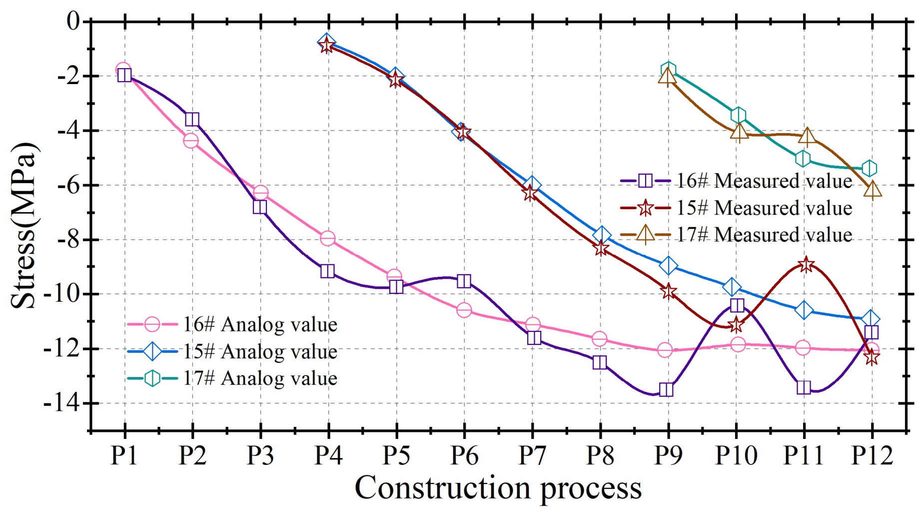

(a) The upper structure of the main bridge

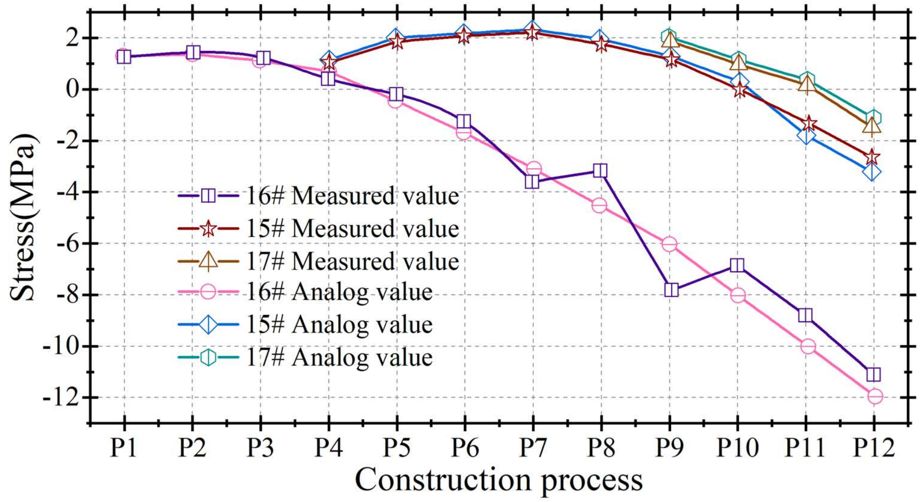

(b) The lower structure of the main bridge

Fig. 6. The stress change trend of the construction process beam segment

4.2. Structural Residual Load Capacity and Interface Slip

4.2.1. Residual structural load capacity. In the previous section, a parametric analysis of the main bridge forces during the demolition of the Clearwater River Bridge was performed, and when the bridge was subjected to chloride ion erosion during service after some of the bridge piers were removed, the concrete degraded with increasing service life. The corrosion of the exposed steel leads to a reduction in the effective thickness, and the susceptibility of the base slab concrete to chloride erosion leads to corrosion of the tensile reinforcement, which can adversely affect the load carrying capacity of the bridge. The deterioration model of concrete and the damage model of steel and reinforcement are introduced into the numerical simulation to establish a time-varying deterioration model of the bridge that can take into account the deterioration of the performance in the service environment, and the load-mid-span deflection curves of the girder bridge at different ages are obtained as shown in Fig. 7.

From the figure, it can be seen that:

1) The load-mid-span deflection curve of the bridge section over the Qingshui River is roughly divided into three stages, when the acting load does not reach the yield load before the first stage, the load and deflection are linearly correlated, and the load corresponding to the turning point is the yield load of the bridge section over the Qingshui River. In the second stage, the slope of the curve gradually decreases, and the stiffness of the bridge section decreases until the curve is close to the horizontal, the structure enters the limit state, and the highest point of the curve corresponds to the load value of the bridge's ultimate bearing capacity. In the third stage, the structure becomes unstable, even if the applied load is not increased, the deformation in the span is getting bigger gradually, and the final result is that the concrete of the top slab is crushed, which leads to the damage of the combined box girder structure.

2) The values of ultimate bearing capacity and corresponding mid-span deflection slightly increased in the first 15 years and gradually decreased in the later stage, and the increase of concrete strength in the early stage was the reason for this result.

3) Under the same load, the bridge mid-span deflection slightly decreased in the first 15 years of action and gradually increased in the later period.

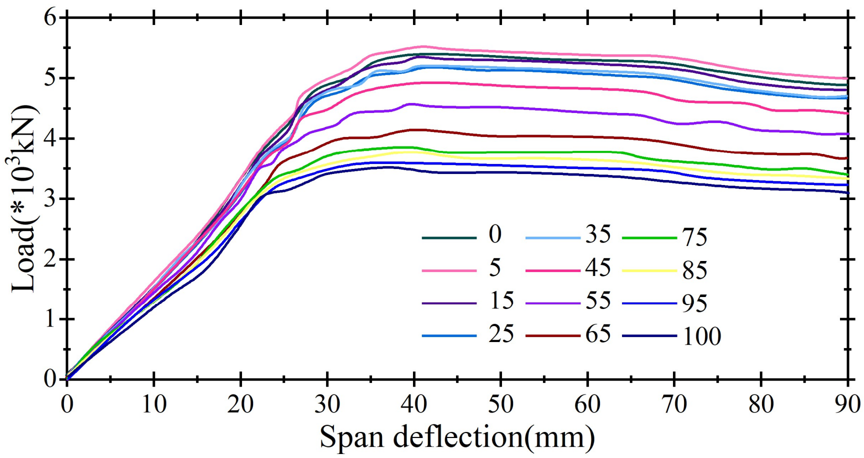

Fig. 7. Load - span deflection curve

The bearing capacity values of the corrugated steel web combined box girder bridge under different ages are summarized into a table, and the specific results are shown in Table 2, according to which each value of the table is analyzed for the residual bearing capacity. From the table, it can be obtained that when the acting load in the span of the bridge section over the Clearwater River is about 80% of its ultimate load, at this time, the lower flange penetration reinforcement yields, the deflection increases, and the combined girder is still in an elastic state. With the continuous increase of the action load, the concrete corresponding to the open rib plate of the shear connection starts to undergo plastic damage, and the plastic neutralization axis of the box girder cross-section moves upward from the corrugated steel web to the interior of the upper flange shear bond and the concrete top plate, resulting in the increase of the strain of the concrete with the excavated holes, and the consequent decrease of the shear bond shear bearing capacity. In reaching the damage state, the bridge span through the reinforcement yielding, concrete top plate with dug holes in the concrete crushed, concrete bottom plate span and support at the transverse penetration cracks, concrete top and bottom plate connection structure did not appear shear damage. And in the first 5 years after the removal of the bridge section of the Clearwater River, the residual bearing capacity of the bridge structure increased slightly, and its value increased from 5.23*103kN to 5.51*103kN, because of the increase in the strength of the concrete caused by the hydration reaction, and at this time the tensile reinforcement did not corrode. With the increase of service time, the residual bearing capacity of the Clearwater River bridge section decreases faster before the first 75 years, and the rate of decrease slows down after 75 years because the corrosion rate of the exposed reinforcement and shear bond slows down in the later period, resulting in a slower decrease in its bearing capacity. This resulted in a slower decline in the remaining structural load carrying capacity of the Clearwater River bridge segment. The ultimate load carrying capacity of the bridge section of the Qingshui River decreased by 25.62% in about 75 years, which shows that the influence of corrosion on the structural load carrying capacity of the bridge section of the Qingshui River should not be neglected.

Table 2. The structural bearing capacity of different years of life

Life span	Yield load (*103kN)	Ultimate load (*103kN)	Load ratio
0	4.54	5.23	0.868
5	4.46	5.51	0.809
15	4.29	5.16	0.831
25	4.01	5.08	0.789
35	3.71	4.89	0.759
45	3.42	4.71	0.726

55	3.23	4.52	0.715
65	3.08	4.07	0.757
75	2.95	3.89	0.758
85	2.91	3.82	0.762
95	2.83	3.74	0.749
100	2.76	3.69	0.738

4.2.2. Interface slip analysis. Under the combined effect of corrosion and fatigue loading, the load-girder end slip curves of the bridge section of the Qingshui River under different ages are shown in Fig. 8. The results show that at the beginning of loading, the interfacial slip of the Qingshuihe bridge section is small, and the growth rate of the slip does not differ much at different ages, and the stiffness gradually decreases as the loading continues. With the increase of time, the performance degradation of Qingshuihe bridge section due to corrosion and fatigue loading is obvious.

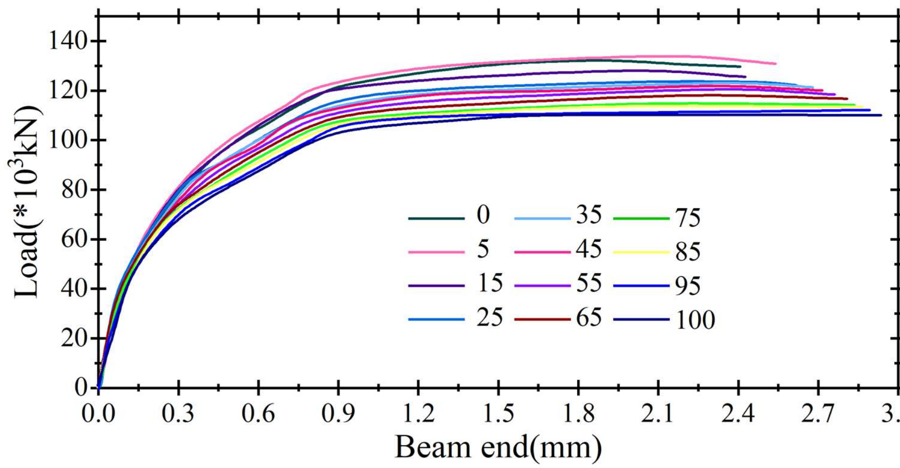

Fig. 8. Load - flow curve

The values of the residual bearing capacity of the Clearwater River bridge segment under different years and the interface slip when reaching the residual bearing capacity are summarized, and their details are shown in Table 3. As shown in the table, at 35 years, the maximum slip of the bridge section of the Qingshui River reached 2.701 mm, which increased by 11.89% compared to the time when it was just removed, and at 75 years, the maximum slip of the bridge section of the Qingshui River reached 2.851 mm, which increased by 18.21% compared to the time when it was just removed. at 100 years, the maximum slip of the bridge section of the Qingshui River reached 2.927 mm, which increased by 21.35% compared to the time when it was just removed. 21.35%. Under the combined effect of corrosion and fatigue loading, both the residual bearing capacity and the interface slip of the Qingshuihe bridge section decreased slightly, which was due to the fact that after the increase of fatigue loading, the concrete, pins, and steel girders were affected, and the pins and steel girders suffered the most obvious effects. At the same time, comparing the slip under different ages, it can be found that the trend of change of slip under the two cases is basically the same, but the growth rate is different, under the joint action of corrosion and fatigue, the growth rate of interface slip is getting bigger and bigger, and it is especially obvious after 65 years, which is because the fatigue damage has a cumulative effect, and the more degradation is more and more obvious at the later stage.

Table 3. Interface slip of Qingshuihe bridge of different ages

Life span	Means Interface (mm)	Residual bearing capacity (kN)
0	1.452	129.38

5	1.583	131.24
15	1.496	124.41
25	1.641	119.56
35	1.683	118.74
45	1.699	117.26
55	1.725	117.03
65	1.746	116.98
75	1.753	115.63
85	1.776	113.24
95	1.812	111.89
100	1.857	110.95

4.3. Calculation of Structural Reliability of Clearwater River Bridge

4.3.1. Structural reliability calculations. Based on the demolition plan of Qingshuihe Bridge given in the previous paper, combined with the formula of structural reliability, the time-varying reliability index of the bridge during the demolition process is calculated by writing a MATLAB program using the JC method. The bridge safety level of Qingshuihe Bridge involved in this paper is Class I, its target reliability is 5.18, and its minimum target reliability index is 4.662 according to the principle of 90% guarantee rate, thus, the calculation results of time-varying reliability indexes in the demolition process of the Qingshuihe Bridge with the help of the JC method are shown in Table 4, and the trend of its change is shown in Fig. 9.

As can be seen from Table 4 and Fig. 9, the calculated value of reliability index of Qingshuihe Bridge changes relatively slowly in the early stage (before 55 years), and starts to decline gradually in the late stage (after 55 years), and the decline speed is getting faster and faster, and it has been reduced to a negative value in the absence of reaching the design base period of 100 years. Through the analysis, it can be obtained that the change of concrete strength and the loss of steel girder cross-section have less influence on the reliability index, while the degradation of steel girder strength has a great influence on the value of the bridge reliability index. During the first 65 years of service, the calculated value of the bridge reliability index is greater than the target reliability index value specified in the code, indicating that it is safe at this time and the bridge fully meets the service requirements. In the use of 75 years, the bridge reliability index value has been less than the minimum target reliability index value of 4.662, indicating that the bridge has been damaged seriously, has not met the normal safety requirements of the bridge, so it is recommended to repair and reinforcement or demolition and reconstruction. In the period of 70~80 years, when the calculated reliability index value is greater than the minimum target reliability index but less than the target reliability index, it means that although the bridge has some damage, it can still be used.

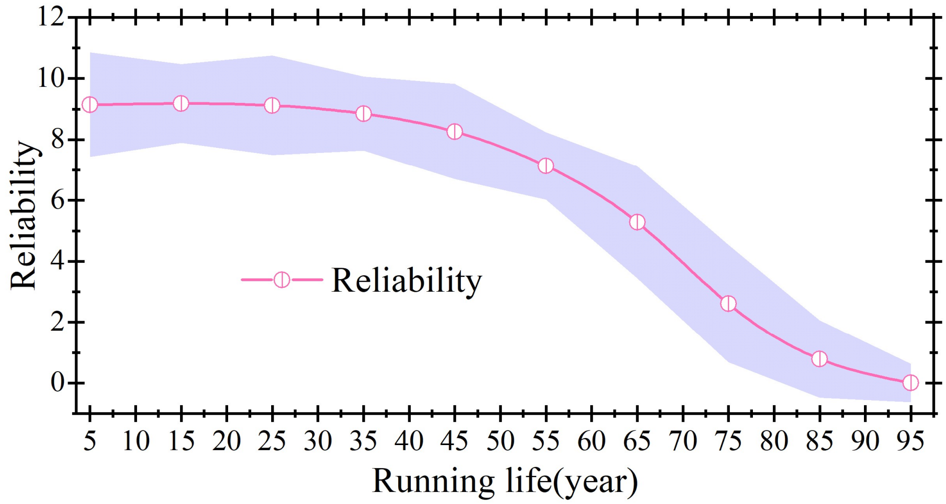

Fig. 9. Calculation results of time-varying reliability

Table 4. The time-variation reliability index of bridge

Life span	5	15	25	35	45
Reliability	9.14	9.18	9.12	8.85	8.26
Life span	55	65	75	85	95
Reliability	7.13	5.28	2.61	0.79	/

4.3.2. Reliability influencing factors. Based on the previous analysis, the factors affecting the time-varying reliability of the structure of the Qingshuihe Bridge mainly include concrete strength, steel girder cross-section loss, and steel girder strength (BS), which are not discussed in this paper due to the relatively small influence of concrete strength and steel girder cross-section loss on the time-varying reliability. The steel girder strength directly affects the size of the resistance during the demolition process of the Qingshuihe Bridge, therefore, the time-varying reliability of the structure of the Qingshuihe Bridge with different steel girder strengths is calculated, and the time-varying reliability is obtained with the time-varying relationship curves as shown in Fig. 10.

From the figure, it can be seen that the time-varying reliability indexes of the combined girders of the bridge with different steel girder strengths have basically the same trend over time, and the magnitude of the decrease is also more or less the same. For the combination girders with steel girder strength greater than 1 and complete shear connection of Qingshuihe Bridge, the reliability indexes in the early stage (25 years ago) are identical, but the time point when the time-varying reliability indexes start to decrease significantly is different, the greater the steel girder strength, the later the time when the time-varying reliability indexes start to decrease significantly. When the strength of steel girder is 0.6, the time-varying reliability index in the early stage is lower than that of the combination girder with full shear connection, and the time point when it starts to decline is the same as that of the combination girder of the Clearwater River Bridge with the strength of steel girder of 1.2, and the time-varying reliability index is declined sharply after the pegs start to corrode. Meanwhile, it can be seen from the figure that the greater the strength of steel beams, the longer the durability service life of the combined beams of the Clearwater River Bridge. Therefore, in the structural durability design of Qingshuihe Bridge after dismantling, full shear connection combination girders with high strength steel girders should be adopted as much as possible, so as to ensure that Qingshuihe Bridge can still maintain good reliability after dismantling part of the piers, which can guarantee the safety of transportation.

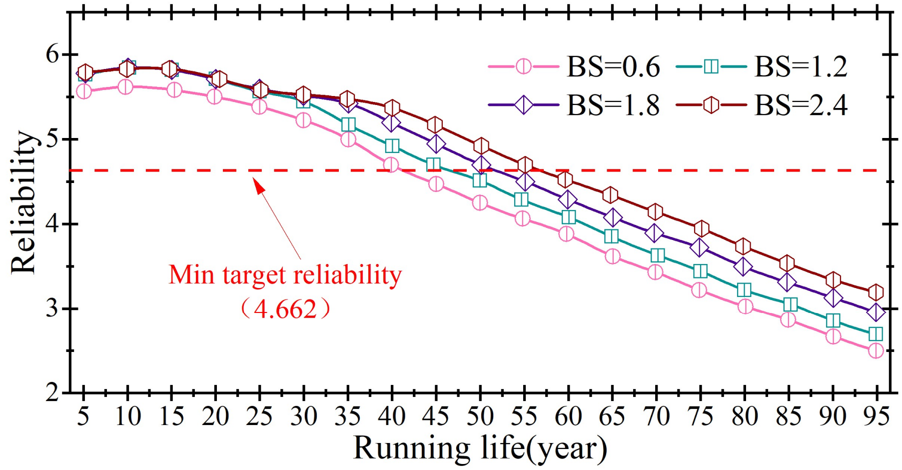

Fig. 10. The time-varying reliability of different steel beams

5. Conclusion

The distribution of the residual bearing capacity of the bridge during the demolition of the Clearwater River Bridge was analyzed by numerically accurate calculations. The conclusions are as follows:
1) The error between the values obtained by finite element simulation and the experimental values of cracking load is relatively small, and its fluctuation range is between 2.12%% and 6.58%, and the finite element simulation value of the bridge over the Qingshuihe Bridge will be a little lower than the experimental values of cracking load under the same conditions of mid-span displacement.
2) The substructure of the waterside section of the main bridge of the Qingshuihe Bridge is in the state of full-section compression during the bearing process, and the value of cross-section positive stress increases with the construction progress, and its shear stress increases with the construction progress.
3) In the first 5 years after the demolition of the bridge section over the Qingshui River, the value of the residual bearing capacity of the bridge structure increased from 5.23*103kN to 5.51*103kN, and its structural residual bearing capacity declined faster before 75 years, and the decline slowed down after 75 years.
4) The value of reliability index of Qingshui River bridge changes relatively slowly in the early stage, and starts to decline gradually in the later stage, and the rate of decline is getting faster and faster, and it has been reduced to negative value when it has not reached the design base period of 100 years, and the greater the strength of steel beams, the higher the time-varying reliability index of the bridge of Qingshui River is.

Funding

This work was supported by Research on Key Technologies for Uninterrupted Navigation, Cross Canal Multi porous Continuous Beam Demolition, and Tied Arch Bridge Reconstruction (SGJLGSKY-2024-01).

References

[1] Guozhen, H., Bo, Y., & Zan, Y. (2019). Damage model test of prestressed T-beam under explosion load. IEEE Access, 7, 135340-135351.

[2] Xu, J., Wu, H., Ma, L., & Fang, Q. (2023). Experimental and numerical study on the residual axial capacity of RC bridge piers after contact explosion. Journal of Bridge Engineering, 28(6), 04023031.

[3] Li, Y., & He, S. (2018). Research of Steel‐Concrete Composite Bridge under Blasting Loads. Advances in

Civil Engineering, 2018(1), 5748278.

[4] Ma, L. L., Wu, H., Fang, Q., & Xu, J. P. (2022). Displacement-based blast-resistant evaluation for simply-supported RC girder bridge under below-deck explosions. Engineering Structures, 266, 114637.

[5] Kong, W., Yang, S., Wang, S., Liu, Z., Zhang, R., Zhong, W., & Yao, X. (2023, May). On dynamic response and damage evaluation of bridge piers under far-field explosion loads. In Structures (Vol. 51, pp. 985-1003). Elsevier.

[6] Liu, L., Zong, Z. H., & Li, M. H. (2018). Numerical study of damage modes and assessment of circular RC pier under noncontact explosions. Journal of Bridge Engineering, 23(9), 04018061.

[7] Lv, C., Yan, Q., Li, L., & Li, S. (2023). Field test and probabilistic vulnerability assessment of a reinforced concrete bridge pier subjected to blast loads. Engineering Failure Analysis, 143, 106802.

[8] Xie, M., Xu, W., Wang, J., Chen, Y., Zhou, D., Hou, L., & Yan, Q. (2023). Preliminary Study on the Damping Effect of a Rotational Inertia Particle Damper Considering the Explosion Response of Continuous Concrete Bridges. Buildings, 13(7), 1726.

[9] Su, Q., Dai, C., & Xu, C. (2018). Full-scale experimental study on the negative flexural behavior of orthotropic steel–concrete composite bridge deck. Journal of Bridge Engineering, 23(12), 04018097.

[10] Lin, J., Zong, Z., Gan, L., Chen, Z., & Li, M. (2023). Damage modes and residual capacity of strand cables subjected to blast loads. Journal of Constructional Steel Research, 204, 107855.

[11] Mi, Y., Ren, H., Sun, C., Zhao, J., Wang, W., Yang, Z., & Chen, Y. (2024). Dynamic behavior and residual performance of CFDSTCs under coupled collision and blast loads. Case Studies in Construction Materials, e04147.

[12] Ma, L. L., Wu, H., & Fang, Q. (2023). Blast-resistant design approach for RC bridge piers. International Journal of Impact Engineering, 180, 104685.
Zhang, C., Gholipour, G., & Mousavi, A. A. (2020). Blast loads induced responses of RC structural members: State-of-the-art review. Composites Part B: Engineering, 195, 108066.

[13] Yang, S., Zhong, W., Wang, S., Kong, W., Tang, Z., Tian, Z., ... & Yao, X. (2022, July). On dynamic analysis and damage evaluation for bridge girders under high-energy air burst. In Structures (Vol. 41, pp. 1488-1500). Elsevier.

[14] Kwaffo, I., Abdallah, M. H., & Braimah, A. (2022, June). Experimental assessment of the residual capacity of axially loaded blast-damaged square RC columns. In Structures (Vol. 40, pp. 469-484). Elsevier.

[15] Bagherzadeh Azar, A., & Sari, A. (2024). Failure analysis and structural resilience of a masonry arch Bridge subjected to blast loads: The Case study, Halilviran Bridge. Mechanics of Advanced Materials and Structures, 1-24.

[16] Xu, K., Sheng, S., Jiang, R., & Feng, Q. (2024). An Experimental Study of the Flexural Bearing Capacity of Reinforced Concrete Beams Damaged by Explosions Using Piezoelectric Smart Aggregates. Sensors, 24(24), 7944.

[17] Zhuo Dong,Yingxian Lang,Bin Gong,Ruifu Yuan,Zhengzhao Liang,Shanyong Wang & Chun'an Tang. (2024). Study on the energy evolution process and damage constitutive model of concrete–granite composite specimens under uniaxial compression load. Geomechanics and Geophysics for Geo-Energy and Geo-Resources(1),194-194.

[18] Li Ping,Li Shan,Zhu Weijun & Lu Yiyan. (2022). Experimental research on the mechanical properties of steel fiber recycled aggregate concrete subjected to true triaxial compression. Construction and Building Materials.

[19] M. Bosco,A. Floridia,D. Panarelli & P.P. Rossi. (2025). A new uniaxial material model for the simulation of

lateral buckling of steel rebars. Engineering Structures(PB),119293-119293.

[20] Abasiodiong Jackson,Simon Fletcher & Nemwel Ariaga. (2024). ANSYS Modelling of Piezoelectric Smart Beam using Ritz Vector Method and Sub-structuring Analysis. Journal of Physics: Conference Series(1),012005-012005.

[21] Ricardo B. Flores & Dante Tolentino. (2024). Reliability assessment of RC bridges considering cumulative damage due to seismic loads. Structures107338-107338.